J|A|C|S ARTICLES

Published on Web 05/21/2009

$BaHg_2Tl_2$. An Unusual Polar Intermetallic Phase with Strong Differentiation between the Neighboring Elements Mercury and Thallium

Jing-Cao Dai,[†,||] Shalabh Gupta,[†] Olivier Gourdon,[‡] Hyun-Jeong Kim,[§] and John D. Corbett*[,†]

Ames Laboratory and Department of Chemistry, Iowa State University, Ames, Iowa 50011, Neutron Scattering Science Division, Oak Ridge National Laboratory, Oak Ridge, Tennessee 37831, and Lujan Neutron Scattering Center, Los Alamos National Laboratory, Los Alamos, New Mexico

Received March 17, 2009; E-mail: jcorbett@iastate.edu

Abstract: High yields of the novel $BaHg_2Tl_2$ are achieved from reactions of the appropriate cast alloys at ~400 °C. (Isotypic $SrHg_2Tl_2$ also exists.) The tetragonal barium structure ($P4_2/mnm$, a = 10.606 Å, c = 5.159 Å) was refined from both single-crystal X-ray and neutron powder diffraction data in order to ensure the atom site assignments although distances and calculated atom site population also support the results. The Hg and Tl network atoms are distinctive in their functions and bonding. Parallel chains of Hg hexagons and of Tl tetrahedra along c are constructed from polyhedra that share opposed like edges, and these are in turn interconnected by Hg−Tl bonds. Overall, the number of Tl−Tl bonds per cell exceeds the Hg−Hg type by 20:12, but these are ~1:2 each in bonding according to their average -ICOHP values (related to overlap populations). Barium is bound within a close 15-atom polyhedron, 12 atoms of which are the more electronegative Hg. LMTO-ASA calculations show that scalar relativistic effects are particularly important for Hg 5d−6s mixing in Hg−Hg and Hg−Tl bonding, whereas relatively separate Tl 6s and 6p states are more important in Tl−Tl interactions. The 6p states of Hg and Tl and 5d of Ba define a dominant conduction band around E_F, and the phase is metallic and Pauli-like paramagnetic. The thallium characteristics here are close to those in numerous alkali-metal−Tl cluster systems. Other active metal−mercury phases that have been studied theoretically are all distinctly electron-richer and more reduced, and without appreciable net 5d, 6s contributions to Hg−Hg bonding.

Introduction

The change from classical Zintl (valence) compounds constructed from active metals and Group 14 to 16 elements to what can be termed electron-poorer Zintl phase precursors has proven to be very productive of new chemistry. The first step, to compounds between the alkali (A) or alkaline-earth (Ae) metals with the heavier triels (Tr = Ga, In, Tl), has led to many unprecedented intermetallic phases, all of which feature more delocalized bonding in polyanionic clusters or networks rather than classical 2c,2e bonding motifs.[1,2] Access to a still electron-poorer derivative of these through substitution of earlier metals into the triel binaries has proven to be exceptionally productive, for gold in particular. The presence of short and evidently strong Au−Tr bonds has become a common feature of numerous tightly packed polar (A, Ae)−Tr−Au intermetallic products, many of which also exhibit novel structure types, and recent explorations indicate similar effects are shown by gold's sixth-period neighbors Pt and Hg. New examples from our investigations include Ba_2AuTl_7,[3] $BaAuTl_3$,[4] KAu_4In_6 and others with novel tunnel structures,[5] $Ca_4Au_{10}In_3$,[6] Ba(Au,Hg)(In,Tl),[7] $AeAu_2In_2$,[8] $BaPtIn_3$,[9] $BaIrIn_4$,[10] and $BaHgTl_3$, $BaHgIn_3$, $BaTl_4$ and $Ba_3Au_4Tl_7$.[11] (Many more unusual compounds and structures are found when the boundaries are expanded to include the rare-earth elements and other transition metals, as with the plumbides.[12]) These sixth period elements are of course famous for large relativistic effects on bonding and stability, and, examples of compounds with some form of gold−gold bonding are especially widely distributed in the general literature.[13,14] The present article describes an especially unusual and appar-

[†] Iowa State University.
[‡] Oak Ridge National Laboratory.
[§] Los Alamos National Laboratory.
[||] Current address: Institute of Materials Physical Chemistry, Huaqiao University, Xiamen, Fujian 361021, China.

(1) Corbett, J. D. *Angew. Chem., Int. Ed.* **2000**, *39*, 670.
(2) Belin, C. H. E.; Tillard-Charbonnel, M. *Prog. Solid State Chem.* **1993**, *22*, 59.
(3) Liu, S. F.; Corbett, J. D. *Inorg. Chem.* **2004**, *43*, 2471.
(4) Liu, S. F.; Corbett, J. D. *Inorg. Chem.* **2004**, *43*, 4988.
(5) Li, B.; Corbett, J. D. *J. Am. Chem. Soc.* **2006**, *128*, 12392.
(6) Lin, Q.; Corbett, J. D. *Inorg. Chem.* **2007**, *45*, 8722.
(7) Dai, J.-C.; Corbett, J. D. *Inorg. Chem.* **2006**, *45*, 2104.
(8) Dai, J.-C.; Corbett, J. D. *Inorg. Chem.* **2007**, *46*, 4592.
(9) Palasyuk, A.; Corbett, J. D. *Z. Anorg. Allg. Chem.* **2007**, *633*, 2563.
(10) Palasyuk, A.; Corbett, J. D. *Inorg. Chem.* **2008**, *47*, 3128.
(11) Dai, J.-C.; Corbett, J. D. unpublished research.
(12) Pöttgen, R.; Rodewald, U. Ch. In *Handbook on the Physics and Chemistry of Rare Earths*; Gschneider, K. A., Jr., Bunzli, J.-C. G., Pecharsky, V. K., Eds; Elsevier: Amsterdam, 2008; Vol.38, p 55.
(13) Pyykkö, P. *Chem. Rev.* **1988**, *88*, 563.
(14) Chem. Soc. Rev. (2008) *37*, topical issue 9.

ently significant example encountered when our explorations included both of the neighboring elements Hg and Tl.

Experimental Section

Syntheses. These were carried out by customary procedures[3−10] via reactions of weighed amounts of the high purity elements that had been welded within 6−9-mm o.d. Ta tubing containers and in turn sealed in evacuated fused silica jackets. All materials were handled in a glovebox filled with dry nitrogen. The metals were dendritic Ba (3−9′s), granular Tl (5−9′s) (both from Alfa-Aesar), and instrument grade Hg (Fisher Scientific). The mixed elements were generally reacted at 730 °C for one day and quenched in water. The resulting finely divided alloy mixture therein was annealed at 400 °C for 7 days and then cooled at 0.5 °C/h to 160 °C. The new $BaHg_2Tl_2$ was first encountered in a $BaHg_2Tl_3$ composition designed to explore the phase width of a new $BaHgTl_3$ ($C2/m$, $SrIn_4$ type).[11] After its X-ray structural analysis, silvery single crystals of the indicated $BaHg_2Tl_2$ were obtained as a nearly single phase product after a similar reaction of that composition. The yield was ∼90% by volume as judged by comparison of its Huber (Guinier) powder pattern with those calculated for the possible components (see Figure S1 in the Supporting Information). Attempts to obtain EDX analyses failed because of the high sensitivity of the compound to moist air. ***Caution:*** *Care and forethought should be employed in running reactions of mercury in such Ta containers at elevated temperatures in case the target phase does not form and the container leaks from overpressure. The normal boiling point of Hg is 361 °C, and we have estimated well-constructed Ta containers will readily retain internal pressures of 3−5 atm. Thicker end-caps or multiple folding at the tubing closures may be necessary.*

X-ray Diffraction. Powder diffraction data were collected on a Huber 670 Guinier powder camera equipped with an area detector and Cu $K\alpha_1$ radiation (λ = 1.540598 Å). Finely powdered samples were homogeneously dispersed between flat Mylar films with the aid of vacuum grease. The detection limit of a second phase with this instrument and system is conservatively estimated to be about 5 vol % in equivalent scattering power, so that apparently single phase patterns are concluded to represent >95% phase purity. Refined lattice parameters were obtained from assigned Guinier patterns with the aid of the UNITCELL program[15] $a = b$ = 10.557(2) Å, c = 5.154(2) Å, V = 574.3(2) Å^3 from 26 lines over 2θ = 5−80°. Isotypic $SrHg_2Tl_2$ has also been obtained in low yield by the same procedure; a = 10.417(2) Å, c = 4.952(1) Å, V = 537.4 Å^3 according to a single crystal tuned on the diffractometer. On the other hand, the analogue $BaHg_2In_2$ occurs with the tetragonal $BaAl_4$ structure type, $I4/mmm$.[11]

Single-crystal data from a $BaHg_2Tl_2$ crystal sealed in a glass capillary were collected at room temperature (293(2) K) as 10-s frames up to θ = 29.29°. A Bruker Smart *APEX* CCD-equipped X-ray diffractometer with Mo Kα radiation (λ = 0.71073 Å) was utilized. The reflection intensities were integrated by the *SMART* software package[16] for the indicated tetragonal cell, and the systematic absences analyzed by the *XPREP* program in the *SHELXTL* 6.1 software package[17] suggested $P4_2/mnm$ (No. 136), $P\bar{4}n2$ (No. 118) or $P4_2nm$ (No. 102) as possible space groups. Although the intensity statistics ($|E^2 - 1| = 0.901$) did not give a very clear indication of centricity, refinement of $BaHg_2Tl_2$ proceeded successfully in centrosymmetric $P4_2/mnm$, The data were corrected for empirical absorption with the aid of *SADABS* program.[18] Finally, the structure was solved by direct methods using above program package, and by full-matrix least-squares refinement, ultimately with anisotropic thermal parameters and a secondary extinction correction. This converged at R1 [$I > 2\sigma(I)$] = 4.14%, wR2 = 7.72%, and GOF = 1.005. The largest residual peak and hole in the ΔF map were 3.26 and −3.25 e·Å^{-3} at 1.05 and 0.82 Å from Hg2 and Ba atoms, respectively. The positional and interatomic distance data for $BaHg_2Tl_2$ are listed in Tables 1 and 2, and the remainder of the parameters are in the Supporting Information. Lattice parameters refined from the Huber powder diffraction were used in the distance calculations.

Table 1. Atomic Coordinates and Displacement Parameters (Å^2) for $BaHg_2Tl_2$ from X-ray Refinement ($P4_2/mnm$; a = 10.606(2) Å, c = 5.159(1) Å)

atom	Wyckoff	x	y	z	U(eq)[a]
Tl	8i	0.4711(1)	0.1405(1)	0	0.021(1)
Hg1	4g	0.5957(1)	0.4043(1)	0	0.019(1)
Hg2	4f	0.1858(1)	0.1858(1)	0	0.023(1)
Ba	4g	0.8495(1)	0.1505(1)	0	0.014(1)

[a] U(eq) is defined as one-third of the trace of the orthogonalized U_{ij} tensor.

Table 2. Interatomic Distances in $BaHg_2Tl_2$[a]

bond	distance, Å	bond	distance, Å
Tl−Tl	3.043(2)	Hg(1)−Ba	3.807(2)
Tl−Hg(2)	3.064(2)	Hg(2)−Hg(1)	2.913(1) × 2
Tl−Hg(1)	3.094(1)	Hg(2)−Tl	3.064(2)
Tl−Tl	3.359(1) × 4	Hg(2)−Ba	3.561(2) × 2
Tl−Ba	3.6374(9)	Hg(2)−Ba	3.587(2) × 2
Tl−Ba	3.6374(9) × 2	Ba−Hg(2)	3.561(2)
Tl−Ba	4.014(2)	Ba−Hg(2)	3.561(2) × 2
Hg(1)−Hg(1)	2.870(3)	Ba−Hg(2)	3.587(2) × 2
Hg(1)−Hg(2)	2.913(1) × 2	Ba−Tl	3.6374(9) × 4
Hg(1)−Tl	3.094(1)	Ba−Hg(1)	3.716(1) × 4
Hg(1)−Ba	3.716(1) × 4		

[a] X-ray data.

Although mercury cannot be distinguished from thallium at this X-ray wavelength, the Wyckoff 4g and 4f sites were tentatively assigned to Hg, and the 8i to Tl on the basis of shorter M−M distances between the former, 2.87 Å and 2.91 × 4 Å. These compare well with the 2.82 Å Hg−Hg bond in analogous hexagonal ring in $CaHg_2$,[18] and 2.91−3.05 Å for the smallest Hg−Hg distances among three Na−Hg phases.[20] Likewise, the 3.04 and 3.36 × 4 Å separations between the assigned Tl atoms compare with a 3.27 Å average for the four smallest values in Ba_2AuTl_7,[3] and a range of 2.99−3.17 Å for the eight shortest Tl−Tl separations in the lower symmetry $BaTl_4$.[11] These distance variations above of course depend to some degree on the number of bonded neighbors in each; in the somewhat peculiar $BaHg_2Tl_2$ structure, the Tl atoms have 5Tl + 2Hg neighbors whereas Hg1 has only 3Hg and 2Tl, and Hg2, 2Hg and 2Tl bonded neighbors.

Neutron Diffraction. A neutron powder diffraction study was carried out on ∼1.8 g of $BaHg_2Tl_2$ inasmuch as the elastic neutron cross sections for Hg (20.24 × 10^{-24} cm^2) and Tl (9.678 × 10^{-24} cm^2) should allow refinement of site distributions. Time-of-flight (TOF) neutron diffraction data were collected on the neutron powder diffractometer (NPDF) at the Manuel Lujan Neutron Scattering Center of Los Alamos National Laboratory. The data were collected using the 148°, 119°, 90°, and 46° detector banks, which cover d-spacings from 0.12 to 7.2 Å. The unit cell parameters, atom positions, and isotropic displacement parameters (IDPs) were refined by the Rietveld method with the

(15) Holland, T. J. B.; Redfern, S. A. T. *Mineral. Mag.* **1997**, *61*, 65.
(16) *SMART*; Bruker AXS, Inc.; Madison, WI, 1996.
(17) *SHELXTL*; Bruker AXS, Inc.; Madison, WI, 2000.
(18) Blessing, R. H. *Acta Crystallogr.* **1995**, *A51*, 33.
(19) Iandelli, A.; Palenzona, A. *Atti Accad. Nazl. Lincei Cl. Sci. Fis. Mat. Nat. Rend., Ser. 8* **1964**, *37*, 165.
(20) Deiseroth, H.-J.; Biehl, E.; Rochnia, M. *J. Alloys Compd.* **1997**, *246*, 80.

aid of *Jana2006* software,[21] starting with the refined positions from the X-ray diffraction study. Background coefficients, scale factors, isotropic strain terms in the profile function, and sample absorption were also refined for a total of 29 parameters. To confirm the disposition of Hg and Tl to the three possible Wyckoff sites (above), several occupancy models were used as starting points. Only one among these gave a satisfying refinement ($\chi^2 = 1.66$ for $R_w = 3.22\%$) with Tl at the 8i site and Hg on the other two (4f, 4g), as also deduced from relative distances and site potentials (below). Less than 10% of a heteroatom substitution appeared to be detectable. Accordingly, the "inverse" model converged poorly at a $\chi^2 = 3.02$ for $R_w = 5.33\%$ and yielded some unphysical IDPs. Finally, to confirm the atom distributions, the three Wykoff sites were given mixed Hg/Tl populations, but a few cycles of refinement converged to that first given above and reported for the structure. Table S5 in the Supporting Information summarizes the numerical results, and Figure S2 compares the observed and calculated neutron diffraction patterns for data from the 148° bank of detectors as an example.

Properties. Electrical resistivities of $BaHg_2Tl_2$ were determined at 34 MHz over the range of 80−280 K by means of the electrodeless "Q" method for 85.5 mg of sample with grain diameters between 150 and 250 μm that was dispersed in alumina.[22] The data yield ~70.5 $\mu\Omega\cdot$cm at 298 K with a mean temperature dependence of 3.67% K^{-1}, corresponding to a metal-like behavior (Supporting Information).

Magnetic susceptibilities of a 90.6 mg polycrystalline sample of $BaHg_2Tl_2$ were measured between 1.8 and 350 K with the aid of a Quantum Design (MPMS) SQUID magnetometer. The results are small, positive, and almost temperature- independent over 25−350 K, characteristic of Pauli-type paramagnetism: $\chi_m \approx 3.1 \times 10^{-4}$ emu$\cdot$mol^{-1} at 3 T and $\approx 8.4 \times 10^{-4}$ emu$\cdot$mol^{-1} at 1 T after container and ion core corrections (Supporting Information).

Electronic Structure Calculations. Tight-binding calculations were performed according to the linear muffin-tin-orbital (LMTO) method in the atomic sphere approximation (ASA).[23] The radii of the Wigner−Seitz spheres were assigned automatically subject to a 16% overlap restriction,[24] and additional empty spheres were not necessary. A basis set of Ba 6s/(6p)/5d, Hg 6s/6p/5d/(5f), Tl 6s/6p/5d/(5f) (downfolded orbitals in parentheses) was employed, and the reciprocal space integrations were performed on grids of 135 irreducible *k*-points. Scalar relativistic corrections were included. For bonding analysis, the energy contributions of all filled electronic states for selected atom pairs were calculated by the COHP method (crystal orbital Hamilton population),[25] and these were also integrated up to E_F to give -ICOHP values (Table S6). The two give useful approximations of relative overlap populations (≈bond strengths). The Fermi level is set to zero in all figures.

Results and Discussion

Exploratory syntheses in the Ba−Hg−Tl system following the discovery of $BaHgTl_3$[11] ($SrIn_4$-type[26]) yielded a new phase which by single-crystal X-ray diffraction and its subsequent high yield synthesis was concluded to be $BaHg_2Tl_2$ according to the simplest structural interpretation. The especially remarkable segregation and structural differentiation of the two neighboring components Hg and Tl was first deduced on the basis of observed distances, those for Tl−Tl being larger than for Hg−Hg by 0.1 Å or more in related polar intermetallics (above). This was buttressed by the noticeable differences in calculated site potentials or charge densities among the different lattice sites, a valuable approach that has been used to help sort out "coloring" problems associated with a range of similar heteroatom distributions.[27] These differences appear to be intrinsic characteristics of many complex structures. Thus, an extended Hückel calculation[28] employing the same Hg/Tl average Hückel parameters at all network positions yielded net Mulliken populations (relative to the neutral atoms) of 2.11 (4g), −0.36 (8i), −0.60 (4f), and −0.79 (4g), consistent with their respective assignments to Ba, Tl, Hg2, and Hg1. The association of mercury with the most negative 4-fold sites parallels its distinctly larger Mulliken electronegativity ((EA+ I)/2): Hg 4.91, Tl 3.2, Ba 2.2 eV[29]), which in turn reflects the electronic differences between Hg ($5d^{10}6s^2$) and Tl ($5d^{10}6s^26p^1$), particularly for their relative 5d,6s orbital energies according to relativistic effects[13] (below). The tentative structural model developed according to these two bits of evidence regarding Wykoff site assignments was verified in all respects from the neutron diffraction data for powdered $BaHg_2Tl_2$ collected at the Lujan Center at the Los Alamos National Laboratory. Alternate assignments all gave clearly inferior refinements (above).

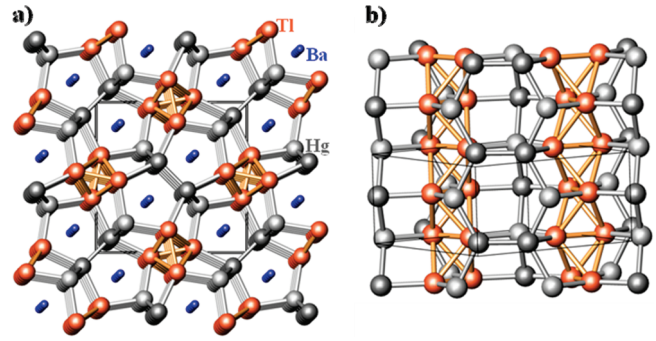

Figure 1. Crystal structure of tetragonal $BaHg_2Tl_2$, with Tl shown as orange, Hg as silver (two kinds), and Ba as blue spheres. (a) [001] view along condensed Tl and Hg chains; (b) ~[110] side view of chains of condensed Tl tetrahedra (along vertical 4_2 axes) together with opposed pairs of zigzag chains of alternating Hg1 (darker) and Hg2 that are condensed into parallel chains of Hg hexagons.

The Structure. Figure 1 shows orthogonal views of this striking tetragonal structure of $BaHg_2Tl_2$ according to the correct assignments of Hg (4e, 4f sites, silver) and Tl (8i, orange). The elements appear functionally well segregated. The thallium (orange) define infinite columns of tetrahedra that share short (3.01 Å) trans-edges along 4_2 axes that center the side faces of the tetragonal cell, Figure 1a. Parallel chains of mercury hexagons (silver) that share trans edges are positioned along 2-fold inversion axes (0, 0, *z;* 1/2, 1/2, *z*, etc.) between the tetrahedral Tl columns, Figure 1b. (The overall Hg units are generated via short bonds (2.97 Å) between pairs of opposed zigzag Hg chains of alternating Hg1 (darker) and Hg2 atoms.) Each type of chain projected along *c* shows alternate 90°

(21) Petricek, V.; Dusek, M.; Palatinus, L. *The Crystallographic Computing System JANA2006*; Institute of Physics: Praha, Czech Republic; 2006.
(22) Zhao, J.-T.; Corbett, J. D. *Inorg. Chem.* **1995**, *34*, 378.
(23) Tank, R.; Jepsen, O.; Burkhardt, A.; Andersen, O. K. *TB-LMTO-ASA Program, Version 4.7*; Max-Planck-Institut für Festkörperforschung: Stuttgart, Germany 1995.
(24) Jepsen, O.; Andersen, O. K. *Z. Phy. B* **1995**, *97*, 35.
(25) Dronskowski, R.; Blöchl, P. E. *J. Phys. Chem.* **1993**, *97*, 8617.
(26) Seo, D.-K.; Corbett, J. D. *J. Am. Chem. Soc.* **2002**, *124*, 415.
(27) Miller, G. J.; Lee, C.-S.; Choe, W. In *Inorganic Chemistry Highlights*; Meyer, G., Naumann, D., Wesemann, L., Eds.; Wiley-VCH: Weinheim, Germany, 2002; p 21.
(28) Ren, J.; Liang, W.; Whangbo, M.-H. *CAESAR for Windows*; Prime-Color Software, Inc., North Carolina State University: Raleigh, NC, 1998.
(29) Pearson, R. G. *Inorg. Chem.* **1988**, *27*, 736.

rotations, Figure 1a. As a result, each chain type is bonded to four of the other kind via intermediate length Hg−Tl bonds, 3.06−3.09 Å. The observed Hg−Hg separations average about 0.4 Å less than those for Tl−Tl, in accord with other examples in similar polar intermetallic compounds.[3,4,7,11] The environment of barium is typical (Figure S3, Supporting Information); it centers a pentagonal prism defined by six Hg and four Tl that is further bounded around the waist by a distorted ring of seven coplanar Hg/Tl atoms, but only three Hg in the latter are within reasonable bonding distances. The distribution of nearer neighbors around barium appears appropriate considering the implied polarity of this phase, nine Ba−Hg distances at 3.59−3.86 Å (3.67 Å average) as opposed to four Ba−Tl contacts of 3.64 Å.

Electronic Structure. The results of scalar relativistic LMTO calculations give us a good deal of insight into what factors makes this compound well bound and so distinctive. In essence, relativistic effects are more important for the smaller Hg, leading to significant mixing of bonding with its 5d and 6s states, whereas 5d−6s effects appear substantially less for Tl, rather 6s and 6p are more responsible for its bonding. These can be sorted out with the aid of the four plots in Figure 2 as a function of energy: (a) total densities-of-states (DOS) (black) with the Ba, Hg, and Tl projections as blue, green, and red lines, respectively; (b) the orbital breakdown of DOS for Tl (red) in terms of 5d, 6s, and 6p components as solid, dotted, and dash-dotted curves, respectively (plus total Ba in blue); (c) the corresponding 5d, 6s, 6p components of Hg in green; and (d) the -COHP data (≈overlap populations) in eV per bond for Hg−Hg (green), Tl−Tl (red), and Hg−Tl (black) contacts. The most prominent features in the DOS (a) are the narrow Tl 5d (red) and a broader Hg 5d (mainly) (green) bands separated by ∼2.5 eV, above which a pair of large, mainly s- and p-based features extend beyond E_F (dashed line). The orbital breakdowns for Tl and Hg in frames (b) and (c) enable most of the foregoing components to be assigned fairly unambiguously. (Separate plots for each orbital type are given in Supporting Information, Figure S4.) Only relatively small amounts of Ba 5d and Tl 6s states lie within the Tl 'd band', as judged from orbital components appearing at the same energy, whereas substantial Hg 6s and nearly as many Tl 6s states appear within the large Hg 'd band', principally in the less tightly bound portion. (The 5d−6s association for Hg reflects their smaller 5d−6s energy separation because of (scalar) relativistic effects. Omission of this correction in the calculation opens up a gap of nearly 2 eV.)

The nature of bonding in the broad area of higher lying states (∼ −6.5 to −2.5 eV) that largely originate from Hg 6s and Tl 6s becomes clearer from the -COHP data, below. In addition, an interesting, isolated group of Tl 6s contributions around −9 eV evidently represent a novel Tl 6s band along (and between) the $Tl_{4/2}$ chains, Figure 1b. (This integrates to two electrons per formula unit.) Finally, substantially all of the group of states between about −2 eV and E_F originate with Tl 6p, somewhat smaller Hg 6p contributions, and an appreciable number of Ba 5d states as well. In fact, some Ba 5d, 6s, and 6p states all mix into the Hg 5d band and higher (Figure 2a), the overall effect reflecting some clear covalency between the nominal cation and anionic components. DOS projections of the separate Ba orbitals are in Supporting Information, Figure S5. Appropriately, $BaHg_2Tl_2$ was shown to be Pauli-paramagnetic and metallic in resistivity, ∼70.5 $\mu\Omega\cdot$cm at 298 K (Supporting Information).

The -COHP results for the principal pairwise atom interactions in $BaHg_2Tl_2$ as a function of energy, Figure 2*d*, and their -ICOHP integrands (Table S6, Supporting Information) afford

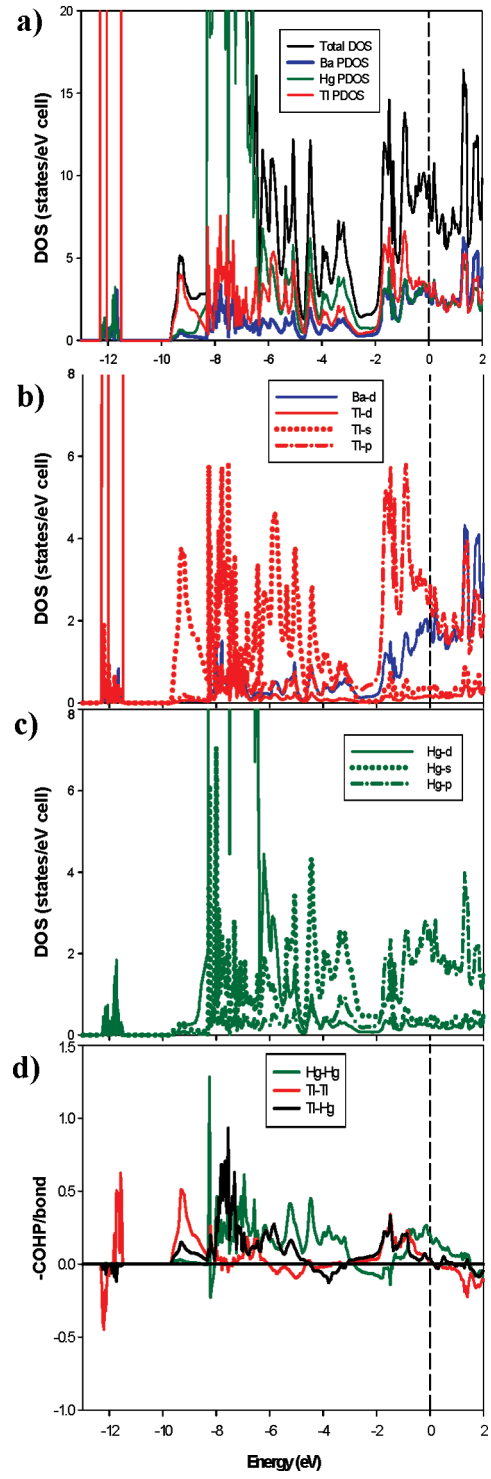

Figure 2. Theoretical results of LMTO-ASA calculations on tetragonal $BaHg_2Tl_2$. (a) Densities-of-states (DOS) for different atom types as a function of energy (eV): black, total, and atomic projections as blue, Ba; green, Hg; red, Tl. (b) Partial Tl (red) projections of separate 5d, 6s, 6p components as solid, dotted, and dashed lines, respectively; Ba in blue. (c) Hg 5d, 6s, 6p projections (green) as solid, dotted and dashed lines, respectively. (d) -COHP values (eV per bond) for all Tl−Tl (red), Hg−Hg (green), and Hg−Tl (black) interactions as a function of energy. These occur 20, 16, and 12 times per cell, respectively.

useful assessments of the relative number and kinds of bonding interactions present. Appreciable bonding contributions occur across most of the energy scale, reasonably increasing in binding

energy from Tl−Tl to Tl−Hg to Hg−Hg. Coincidence of the last two within the so-called Hg '5d band', which spans about −8.5 to −6.5 eV, are, in increasing energy, Hg 6s (the sharp green spike), mainly Tl 6s (not 5d, black) and Hg 6s (green) above the novel sub-band around −9 eV of Tl 6s mixed with a little Tl−Hg interchain component. On the other hand, the Tl−Tl contributions between ∼ −6 and −3 eV are slightly antibonding, in spite of the density of Tl 6*s* states in this region, Figure 2b. The so-called $BaHg_2Tl_2$ 'p-band' above ∼ −2 eV is distinctive indeed, first, in terms of similar Tl−Tl and Tl−Hg 6p bonding components and, nearer E_F and beyond, mainly Hg−Hg 6p bonding. The emphasis on only 6s and 6p bonding for Tl is clear.

In terms of structural differentiations, mercury with its peculiar substructure has the lowest number of bonded Hg and Tl neighbors, four (Hg2) or five (Hg1), compared with seven neighbors about each Tl. The numbers of total Tl−Tl, Tl−Hg, and Hg−Hg contacts per cell in turn vary as 20:16:12, whereas the average -ICOHP values for each bond type increase in parallel, 0.69:1.02:1.29, (although the latter are not quantitatively intercomparable), and the average bond lengths, least indicative of bonding trends, decrease in the same order, as perhaps expected (Table S6). The overall -ICOHP sums then vary as 13.8 to 16.3 to 15.5 eV per cell for Tl−Tl, Tl−Hg, and Hg−Hg, respectively, although these too are a bit of "apples and oranges" in close intercomparisons. The geometries of the Hg and Tl substructures and the relatively low number of cations remain the most distinctive features.

Other Examples. Two other recent LMTO studies on electron-richer intermetallics with Au−Au or Hg−Hg bonding[30,31] allow some useful comparisons, as well as contrasts, with $BaHg_2Tl_2$ in which up to two electrons per formula unit are formally donated to the network (corresponding to an average oxidation state of −0.5 each for Hg and Tl). In NaHg, rectangular Hg_4 units share opposed edges to generate parallel, well-separated zigzag ribbons, now with up to one more electron per pair of network atoms in comparison. The phase exhibits a lower lying 5d band, about 75% as wide as found here, a splitting of the 6s band of the Hg−Hg bonds into σ_s and σ_s* components, and direct filling of a 6p band. (Na 4s, 4p, 3d states are also involved.)[30] No antibonding 6s effect was found in the present work.

Recent calculations on Ca_5Au_4 and Ca_3Hg_2, which both contain only heavy metal dimers, as well as more valence electrons, naturally reflect even greater filling of 6p band states.[31] (The stoichiometries formally correspond to excesses of five and eight electrons above the classical singly bonded metal dimers, respectively; that is, as Au_2 and Hg_2^{2+}.) The 5d states for Au and Hg lie increasingly lower with only minor 6s mixing even in the former, but more importantly, the 6s bands for both the Au and Hg phases are again split into filled σ_s (bonding) and σ_s* (antibonding) components. In the 'p-metals' that result, the 'extra' electrons increasingly populate the metal 6p bands, which now include separate dimer σ_p bonding states. The dimers are perhaps best approximated as singly bonded, but in the presence of appreciable amounts of additional delocalized electrons at higher energies. (Ca 4s, 4p are also important in the higher bands.)

In comparison, the novel network in $BaHg_2Tl_2$ gives us a better look at delocalized network bonding among 5d metal Hg and the neighboring Tl, and in the presence of a lower formal electron excess. Splitting among the multiple Hg−Hg σ bonds is not evident, but a related 6p band is appreciably populated, particularly for Tl. The 5d−6s bands are broad for Hg−Hg but not so for Tl−Tl, a separate 6s band for the latter being a most notable feature (Figure 2b,d). A chemistry from the Tl 5d band seems to have disappeared in general, and a 6s−6p separation that increases through the p-metals also means less hybridization and more p-orbital-only bonding modes. Another feature related to the properties of $BaHg_2Tl_2$ is that a significant number of alkali-metal compounds of Tl (and In) have been found that contain small isolated triel clusters instead, with formal oxidation states per Tr atom near −1 and with internal delocalized bonding schemes that are more-or-less related by Wade's Rules, e.g., Tl_5^{7-}, Tl_6^{6-}, Tl_6^{8-}, Tl_9^{9-}, and Tl_{13}^{11-}, clusters that are often mixed in structures as well.[1,32] Which particular polyanion is obtained within this diverse group of clusters appears to depend primarily on countercation sizes, proportions, and packing, the clusters selection largely resulting from the 'best fit' in a particular lattice, which may include mixed cations.[1,32,33] The singularity found for Tl in the classic NaTl (and NaIn), a Na-stuffed diamond structure of Tl with obvious relative size constraints, likewise exhibits primarily p-orbital bonding, with little 6s in the valence band or 5d in the 6s band.[34] Isoelectronic cluster sequences along the periods, a characteristic of Zintl phases, also follow. Thus, the predicted tetrahedral "Tl_4^{8-}" in Na_2Tl[35] is nominally isoelectronic with the tetrahedral Pb_4^{4-} present in NaPb.[36] Fortunately, LMTO calculations for both phases have been reported by Hafner and co-workers,[37,38] who observed that the heavy metal bands in these two phases show remarkably similar DOS features, which in fact follows long-standing qualitative expectations from general Zintl−Klemm concepts.[39] (The Tl or Pb 6p orbitals also mix appreciably with Na 3s states in these.) These bonding species were in fact concluded to persist into the corresponding liquid alloy systems, the tetrahedral building blocks dominating local configurations.[38] In these senses, the sizable 6p band we find in $BaHg_2Tl_2$, Figure 2, is in accord with expectations

The forgoing results emphasize two important points about the new compound: (1) that relativistic effects for Hg versus Tl bonding are appreciably different, suitably it would appear for their positions in the periodic table, and (2) the presence of dominant 6p valence states for the heavier Tl supports the differentiation between Hg and Tl in function and bonding. We are of course continuing to look for other novel examples in this region of phase space.

Acknowledgment. The authors are indebted to Gordon J. Miller for his interest and helpful insights and to Serge Bud'kov for the magnetic susceptibility data. This research was supported by the Office of Basic Energy Sciences (BES), Materials Sciences Division, U.S. Department of Energy (DOE) and performed primarily in the Ames Laboratory, which is operated for DOE by Iowa State University under Contract No. DE-AC02-07CH11358. This work

(30) Deiseroth, H. J.; Stupperich, A.; Pankaluoto, R.; Christensen, N. E. *Z. Anorg. Allg. Chem.* **1991**, *597*, 41.
(31) Köhler, J.; Whangbo, M.-H. *Chem. Mater.* **2008**, *20*, 2751.
(32) Dong, Z.-C.; Corbett, J. D. *Inorg. Chem.* **1996**, *35*, 2301.
(33) Dong, Z.-C.; Corbett, J. D. *J. Am. Chem. Soc.* **1995**, *117*, 6447.
(34) Schmidt, P. C. *Struct. Bonding (Berlin)* **1987**, *35*, 91.
(35) Hansen, D. A.; Smith, J. F. *Acta Crystallogr.* **1967**, *22*, 836.
(36) Hewaidy, I. F.; Busmann, E.; Klemm, W. *Z. Anorg. Allg. Chem.* **1964**, *328*, 283.
(37) Tegze, M.; Hafner, J. *Phys. Rev. B* **1989**, *39*, 8263.
(38) Hafner, J.; Jank, W.; Holzmannhofer, J. *J. Non-Cryst. Solids* **1992**, *150*, 266.
(39) *Chemistry, Structure, and Bonding of Zintl Phases and Ions*; Kauzlarich, S. M., Ed.; VCH: New York, 1996.

also benefited from the use of NPDF at the Lujan Center at Los Alamos Neutron Science Center, also funded by BES. Los Alamos National Laboratory is operated by Los Alamos National Security LLC under DOE Contract No. DE-AC52-06NA25396.

Supporting Information Available: Two CIF outputs; Tables S1−S4, X-ray structural data and results; Table S5, results from neutron diffraction study; Table S6, -ICOHP data; Figures S1−2, X-ray and neutron powder pattern results; Figure S3, Ba environment in $BaHg_2Tl_2$; Figure S4, separate DOS projections for the orbitals by atom type; Figure S5, DOS projections for Ba orbitals; Figures S6 and S7, resistivity and magnetic susceptibility data for $BaHg_2Tl_2$. This material is available free of charge via the Internet at http://pubs.acs.org.

JA901865D